

Run-up heights of Tsunami along the eastern coast of the Korean Peninsula

Tae-Min Ha[†], Yong-Sik Cho[‡], Moon-Kyu Choi[∞] and Woo-Chang Jeong[§]

[†]Dept. of Civil Eng.
Hanyang Univ., Seoul
133-791, Korea
kevin4324@hanyang.ac.kr

[‡] Dept. of Civil Eng.
Hanyang Univ., Seoul
133-791, Korea
ysc59@hanyang.ac.kr

[∞] Dept. of Civil Eng.
Hanyang Univ., Seoul
133-791, Korea
civil00@hanyang.ac.kr

[§] Hydro-System Engineering Centre
Korea Institute of Water and Environment
Korea Water Resources Corporation, Daejeon,
305-730, Korea
jeongwc@kowaco.or.kr



ABSTRACT

HA, T.-M., CHO, Y.-S., CHOI, M.-K., AND JEONG, W.-C., 2007. Run-up heights of Tsunami along the eastern coast of the Korean Peninsula. Journal of Coastal Research, SI 50 (Proceedings of the 9th International Coastal Symposium), 348 – 352. Gold Coast, Australia, ISSN 0749.0208

Most of finite difference numerical models developed for simulation of tsunami propagation are based on the shallow-water equations. If spatial and temporal grid sizes are properly selected, the leap-frog finite difference scheme gives correct dispersion effects for a constant water depth. If a water depth changes, however, dispersion effects of tsunami can not be accurately considered at every grid point in the whole computational domain. In this study, new dispersion-correction terms are added to the leap-frog scheme with a purpose of considering dispersion effects as a water depth changes on a real topography. To verify the practicality of the improved numerical model, the propagation across the East Sea of the Central East Sea Tsunami occurred on 26th May, 1983 is simulated. Maximum run-up heights are then predicted at several locations. The predicted run-up heights are compared with available field observed data. A very reasonable agreement is observed.

ADDITIONAL INDEX WORDS: *Dispersion Effects, Boussinesq Equations, Shallow-Water Equations*

INTRODUCTION

Several devastating tsunamis triggered by submarine earthquakes have been observed around the Pacific Ocean area during last decades. Especially, nearshore tsunamis may cause huge inundation of coastal area and huge property damage; because it takes a few minutes to reach a coastline and the time to seek refuge from a tsunami attack cannot be enough. For example, the Indian Ocean Tsunami that occurred on December 26, 2004 killed more than 150,000 people in Banda Aceh, Indonesia. The tsunami had attacked Banda Aceh within a few minutes after generation. Thus, residents had not enough time to seek refuge.

Recently, many submarine earthquakes have occurred around the Korean Peninsula (according to the Korea Meteorological Administration, 21 times in 2003, 24 times in 2005 and 17 times in 2006 up to September). Most tsunamis are triggered by earthquakes occurred in subduction zones around the Pacific Ocean area including the East Sea surrounded by Korea, Japan and Russia (see Fig. 1). In the East Sea, the Central East Sea Tsunami that occurred in 1983 caused a huge loss of human lives and huge property damage to not only Japanese coastal area but also Korean and Russian coastal areas. A fundamental way to

prevent unusual tsunami attack is to construct a safe zone along the coastline based on an inundation map developed by simulating historical and probable maximum tsunami events.

In this study, the governing equations are presented and a simple but robust numerical scheme is newly proposed in the next section. Maximum run-up heights along the eastern coast of the Korean Peninsula are predicted and compared with field observed data. Finally, concluding remarks are made.

GOVERNING EQUATIONS

The propagation of tsunamis across an ocean where a local depth is assumed to be relatively much smaller than a wave length may be governed by the linear Boussinesq equations given in Table 1. In Table 1, ζ is free surface displacements, P is the horizontal component of the volume flux in the x – axis direction, Q is the horizontal component of the volume flux in the y – axis direction and h is the total water depth (a sum of still water depth and free surface displacement), respectively and g is the acceleration of gravity. (LIU et al., 1995; CHO and YOON, 1998).

Table 1: Linear Boussinesq Equation

$$\frac{\partial \zeta}{\partial t} + \frac{\partial P}{\partial x} + \frac{\partial Q}{\partial y} = 0 \quad (1)$$

$$\frac{\partial P}{\partial t} + gh \frac{\partial \zeta}{\partial x} = \frac{h^2}{2} \frac{\partial}{\partial x} \left[\frac{\partial}{\partial x} \left(\frac{\partial P}{\partial t} \right) + \frac{\partial}{\partial y} \left(\frac{\partial Q}{\partial t} \right) \right] - \frac{h^3}{6} \frac{\partial}{\partial x} \left[\frac{\partial^2}{\partial t \partial x} \left(\frac{P}{h} \right) + \frac{\partial^2}{\partial t \partial y} \left(\frac{Q}{h} \right) \right] \quad (2)$$

$$\frac{\partial Q}{\partial t} + gh \frac{\partial \zeta}{\partial y} = \frac{h^2}{2} \frac{\partial}{\partial y} \left[\frac{\partial}{\partial x} \left(\frac{\partial P}{\partial t} \right) + \frac{\partial}{\partial y} \left(\frac{\partial Q}{\partial t} \right) \right] - \frac{h^3}{6} \frac{\partial}{\partial y} \left[\frac{\partial^2}{\partial t \partial x} \left(\frac{P}{h} \right) + \frac{\partial^2}{\partial t \partial y} \left(\frac{Q}{h} \right) \right] \quad (3)$$

Table 2: Cho and Yoon's scheme (1998)

$$\frac{\zeta_{i,j}^{n+1/2} - \zeta_{i,j}^{n-1/2}}{\Delta t} + \frac{P_{i+1/2,j}^n - P_{i-1/2,j}^n}{\Delta x} + \frac{Q_{i,j+1/2}^n - Q_{i,j-1/2}^n}{\Delta y} = 0 \quad (8)$$

$$\frac{P_{i+1/2,j}^{n+1} - P_{i+1/2,j}^n}{\Delta t} + gh_{i+1/2,j} \frac{\zeta_{i+1,j}^{n+1/2} - \zeta_{i,j}^{n+1/2}}{\Delta t} \quad (9)$$

$$+ \frac{\gamma}{12\Delta x} gh_{i+1/2,j} \left[(\zeta_{i+1,j+1}^{n+1/2} - 2\zeta_{i+1,j}^{n+1/2} + \zeta_{i+1,j-1}^{n+1/2}) - (\zeta_{i,j+1}^{n+1/2} - 2\zeta_{i,j}^{n+1/2} + \zeta_{i,j-1}^{n+1/2}) \right] = 0$$

$$\frac{Q_{i,j+1/2}^{n+1} - Q_{i,j+1/2}^n}{\Delta t} + gh_{i,j+1/2} \frac{\zeta_{i,j+1}^{n+1/2} - \zeta_{i,j}^{n+1/2}}{\Delta x} \quad (10)$$

$$+ \frac{\gamma}{12\Delta y} gh_{i,j+1/2} \left[(\zeta_{i+1,j+1}^{n+1/2} - 2\zeta_{i,j+1}^{n+1/2} + \zeta_{i-1,j+1}^{n+1/2}) - (\zeta_{i+1,j}^{n+1/2} - 2\zeta_{i,j}^{n+1/2} + \zeta_{i-1,j}^{n+1/2}) \right] = 0$$

Since the effects of frequency dispersion may play some roles when a tsunami propagates over a long distance, they should be included in the governing equations.

The linear Boussinesq equations in Table 1 are reduced over a constant depth as the following equation (e.g. MEI, 1989).

$$\begin{aligned} & \frac{\partial^2 \zeta}{\partial t^2} - gh \left(\frac{\partial^2 \zeta}{\partial x^2} + \frac{\partial^2 \zeta}{\partial y^2} \right) \\ & = \frac{gh^3}{3} \left(\frac{\partial^4 \zeta}{\partial x^4} + 2 \frac{\partial^4 \zeta}{\partial x^2 \partial y^2} + \frac{\partial^4 \zeta}{\partial y^4} \right) \end{aligned} \quad (4)$$

The frequency dispersion term given by the right-hand side term of equation (4) may cause serious numerical difficulty in practice because of higher order derivatives. An alternative way is to solve a set of lower order partial differential equations, that is, the linear shallow-water equations instead of the linear Boussinesq equations. The numerical dispersion induced by the numerical scheme can be manipulated to represent the physical frequency dispersion of the linear Boussinesq equations.

NUMERICAL SCHEME

In this section, the leap-frog finite difference scheme proposed by CHO and YOON (1998) is first summarised. By denoting $P = uh$ and $Q = vh$ as the volume flux components in the x - and y - axis directions, respectively, the linear shallow-water equations can be rewritten in the following form (LIU et al., 1995):

$$\frac{\partial \zeta}{\partial t} + \frac{\partial P}{\partial x} + \frac{\partial Q}{\partial y} = 0 \quad (5)$$

$$\frac{\partial P}{\partial t} + gh \frac{\partial \zeta}{\partial x} = 0 \quad (6)$$

$$\frac{\partial Q}{\partial t} + gh \frac{\partial \zeta}{\partial y} = 0 \quad (7)$$

CHO and YOON (1998) proposed a leap-frog finite difference scheme to discretise equations (5)-(7) in a staggered grid system (Table 2). In the staggered grid system, indices (i, j) and (n)

Table 3: Modified numerical scheme

$$\frac{\zeta_{i,j}^{n+1/2} - \zeta_{i,j}^{n-1/2}}{\Delta t} + \frac{P_{i+1/2,j}^n - P_{i-1/2,j}^n}{\Delta x} + \frac{Q_{i,j+1/2}^n - Q_{i,j-1/2}^n}{\Delta y} = 0 \quad (11)$$

$$\frac{P_{i+1/2,j}^{n+1} - P_{i+1/2,j}^n}{\Delta t} + gh_{i+1/2,j} \frac{\zeta_{i+1,j}^{n+1/2} - \zeta_{i,j}^{n+1/2}}{\Delta x} + \frac{\alpha}{12\Delta x} gh_{i+1/2,j} \left[\zeta_{i+2,j}^{n+1/2} - 3\zeta_{i+1,j}^{n+1/2} + 3\zeta_{i,j}^{n+1/2} - \zeta_{i-1,j}^{n+1/2} \right] \quad (12)$$

$$+ \frac{\gamma}{12\Delta x} gh_{i+1/2,j} \left[(\zeta_{i+1,j+1}^{n+1/2} - 2\zeta_{i+1,j}^{n+1/2} + \zeta_{i+1,j-1}^{n+1/2}) - (\zeta_{i,j+1}^{n+1/2} - 2\zeta_{i,j}^{n+1/2} + \zeta_{i,j-1}^{n+1/2}) \right] = 0$$

$$\frac{Q_{i,j+1/2}^{n+1} - Q_{i,j+1/2}^n}{\Delta t} + gh_{i,j+1/2} \frac{\zeta_{i,j+1}^{n+1/2} - \zeta_{i,j}^{n+1/2}}{\Delta y} + \frac{\alpha}{12\Delta y} gh_{i,j+1/2} \left[\zeta_{i,j+2}^{n+1/2} - 3\zeta_{i,j+1}^{n+1/2} + 3\zeta_{i,j}^{n+1/2} - \zeta_{i,j-1}^{n+1/2} \right] \quad (13)$$

$$+ \frac{\gamma}{12\Delta y} gh_{i,j+1/2} \left[(\zeta_{i+1,j+1}^{n+1/2} - 2\zeta_{i,j+1}^{n+1/2} + \zeta_{i-1,j+1}^{n+1/2}) - (\zeta_{i+1,j}^{n+1/2} - 2\zeta_{i,j}^{n+1/2} + \zeta_{i-1,j}^{n+1/2}) \right] = 0$$

$$\frac{\partial^2 \zeta}{\partial t^2} - C_0^2 \left(\frac{\partial^2 \zeta}{\partial x^2} + \frac{\partial^2 \zeta}{\partial y^2} \right) - C_0^2 \frac{(\Delta x)^2}{12} (1 + \alpha - C_r^2) \left(\frac{\partial^4 \zeta}{\partial x^4} + 2 \frac{\partial^4 \zeta}{\partial x^2 \partial y^2} + \frac{\partial^4 \zeta}{\partial y^4} \right) \quad (14)$$

$$+ (1 + \alpha - \gamma) C_0^2 \frac{(\Delta x)^2}{6} \frac{\partial^4 \zeta}{\partial x^2 \partial y^2} = O\left((\Delta x)^3, (\Delta x)^2 \Delta t, \Delta x (\Delta t)^2, (\Delta t)^3 \right)$$

denote spatial nodes and the time level, respectively.

A new scheme is proposed as listed in Table 3. In equations (12) and (13), the dispersion-correction factors, α and γ , are determined by a relation of depth, spatial grid and time step sizes. If both α and γ take zero and one, respectively, equations (12) and (13) are simplified to CHO and YOON's scheme.

Now, the numerical dispersion generated by the new scheme is investigated. Following the approach suggested by WARMING and HYETT (1974), the Taylor series expansions of variables ζ , P and Q at a point represented by (n, i, j) are applied to equations (11)-(13). To derive a modified equation, all the higher time derivatives are replaced by the corresponding spatial derivatives and the volume flux components, P and Q , are eliminated. After a lengthy algebra, a modified equation for ζ is obtained as equation (14). In equation (14) a uniform grid, $\Delta x = \Delta y$, is used, and $C_0 (= \sqrt{gh})$ and $C_r (= C_0 \Delta t / \Delta x)$ represent the phase velocity of a linear shallow-water wave and the Courant number, respectively. The leading order terms in equation (14) are the same as those in the wave equation. The terms of $O(\Delta x^2)$ and of higher order are the results of numerical discretisation.

Comparing equation (14) with the linear Boussinesq equation (4), these equations are seen to be identical as long as the following relations are satisfied. That is,

$$\alpha = \frac{4h^2 + gh(\Delta t)^2 - (\Delta x)^2}{(\Delta x)^2}, \gamma = \alpha + 1 \quad (15)$$

In IMAMURA and GOTO's scheme (1988), $\alpha = 0$ and $\gamma = 0$, and CHO and YOON's scheme, $\alpha = 0$ and $\gamma = 1$, the following relation is obtained to be equal to the linear Boussinesq equation.

$$(\Delta x)^2 = 4h^2 + gh(\Delta t)^2 \quad (16)$$

If α and γ are chosen according to equation (16), the numerical dispersion generated from the new scheme mimics the frequency dispersion of the linear Boussinesq equation. In CHO and YOON's scheme, however, the spatial grid and time step sizes should be determined by equation (16). Thus, CHO and YOON's scheme has the limitation that spatial grid size and time step size should be changed continuously as the water depth changes. On the contrary, the new scheme uses the constant spatial grid and time step sizes even in area of variable depths. Furthermore, the accuracy of the numerical scheme is a third order like CHO and YOON's scheme.

NUMERICAL SIMULATION

The Central East Sea Tsunami was triggered by an impulsive undersea earthquake of magnitude 7.7 in 1983. It has been recorded as one of most devastating tsunamis occurred in the East Sea during the last century. The numerical model mentioned in the previous section is employed to predict maximum run-up heights along the eastern coast of the Korean Peninsula. Fig. 1 displays the coastline of the East Sea and a brief bottom topography. The Central East Sea Tsunami occurred near Japan and attacked the Korean Peninsula after about 100 mins journey across the East Sea. In numerical simulations, the East Sea is divided into several sub-regions having different spatial and temporal grid sizes and a dynamic linking technique is used between two connected regions with different grid sizes (LIU et al., 1995).

A moving boundary condition is applied along the coastline of the Korean Peninsula to estimate maximum run-up heights. As shown in Fig. 1, the East Sea has a specific bottom topography.

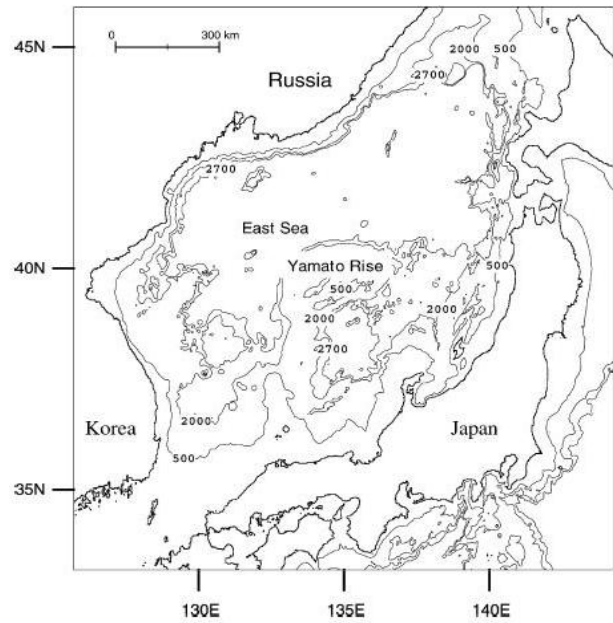


Figure 1. Coastline and bottom topography of the East Sea

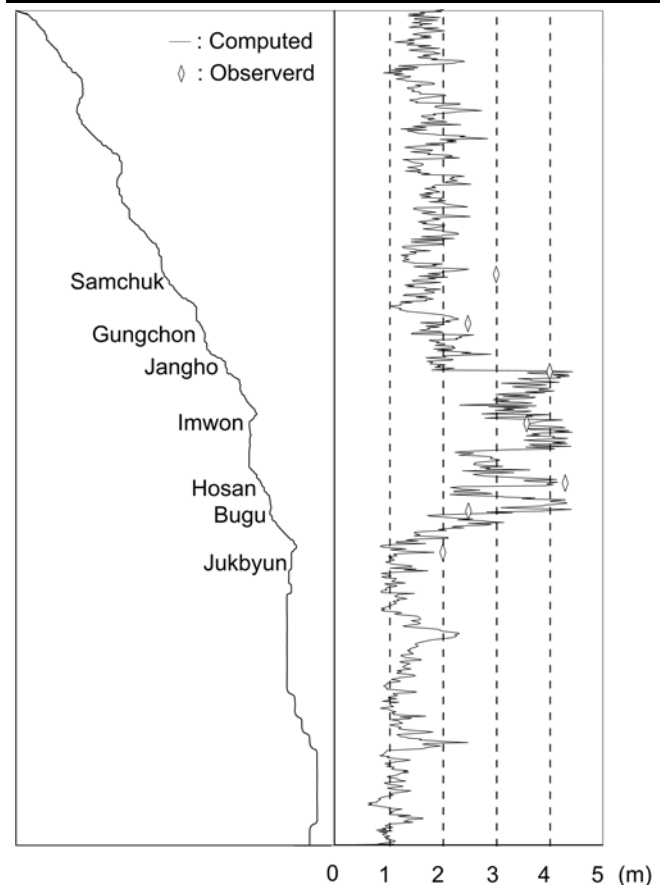


Figure 2. Maximum Run-up heights along the eastern coast of the Korean Peninsula (1st order leap frog finite difference numerical model)

The water depth over the Yamato Rise located about in the centre of the East Sea is less than several hundred metres, while depths

Table 4: Comparison of run-up heights along the eastern coast of the Korean Peninsula

Location	Jukbyun	Bugu	Hosan	Imwon	Jangho	Gungchon	Samchuk
Observed	1.99m	2.47m	4.28m	3.56m	3.99m	2.46m	2.99m
LEE	2.27m	2.15m	3.60m	3.99m	3.12m	2.00m	2.18m
Present study	1.34m	2.74m	4.40m	3.53m	4.28m	2.43m	1.62m

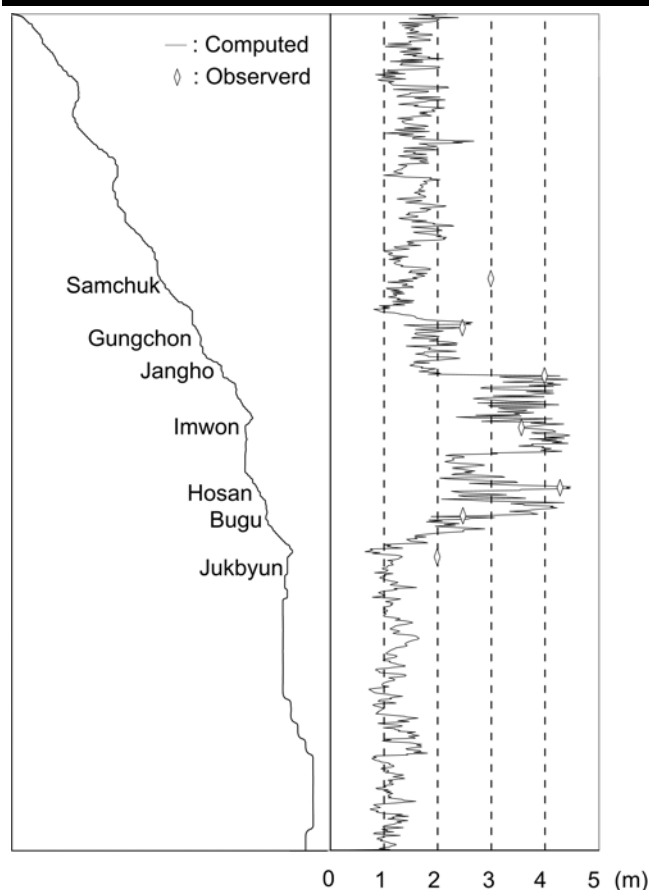


Figure 3. Maximum run-up heights along the eastern coast of the Korean Peninsula (Improved numerical model)

elsewhere are even greater than 2,000m. The number of nodes is $1,170 \times 1,170$ to cover the region shown in Fig. 1. The coarsest grid size is 1.11km in deep water, whereas the finest is 4.6m near the shoreline. Although the model can be run in the spherical coordinate system, the model is run only in the Cartesian coordinate system because effects of the spherical coordinate are negligible in this study (LEE, 1999). The initial profiles of the Central East Sea Tsunami are given in CHO et al. (2004) and not repeated here.

First, wave heights are predicted by using a coarse grid system along the eastern coast of the Korean Peninsula. Compared to observed maximum run-up heights, predicted results are slightly under-estimated. It is thought that even though non-linear shallow water equations are used for computing, shallow water effects are not reproduced well because variation of local topography is not expressed fairly in a coarse grid system. Thus, the tsunami event is re-computed using a finer grid system and got maximum run-up heights. Computed results are compared to previous numerical results and observed (see Fig. 2 and Fig. 3).

Table 4 shows maximum run-up heights at several locations of the Korean eastern coast (see Fig. 3). Maximum run-up heights are

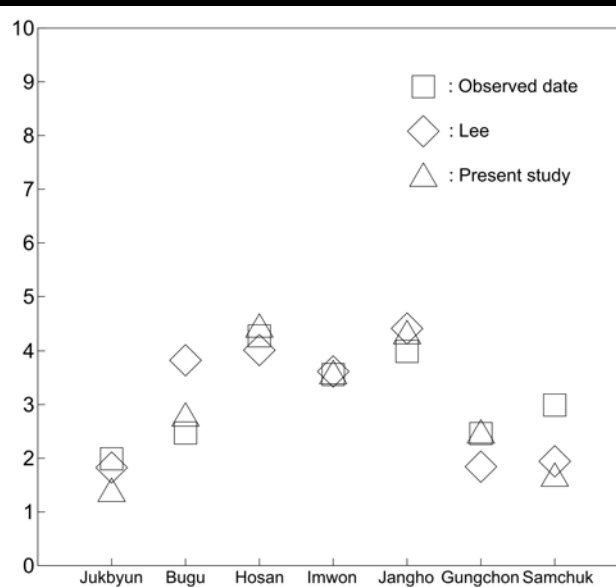


Figure 4. Comparison of run-up heights along the eastern coast of the Korean Peninsula

plotted in Fig. 4 showing comparison with observed data and LEE's. Computed results represent reasonably well maximum run-up heights of the tsunami but Jukbyun and Samchuk are slightly under-estimated. Observed run-up heights are not an averaged value of the wide region but a specific value of the narrow region. It is thought that computed results don't represent reasonably well observed because the model doesn't reproduce characteristics of the land topography.

CONCLUSION

In this study, an improved numerical model has been applied to estimation of run-up heights of tsunamis along the eastern coast of the Korean Peninsula. A target event is the Central East Sea Tsunami. Predicted maximum run-up heights have been compared to the field observed data and that of first-order upwind scheme. Although there is a slight discrepancy, the overall agreement is quite reasonable.

An effective and economic way for minimising losses of human lives and property damage is to construct a safety zone along the coastline based on a maximum inundation map. The map should be developed based on the historical maximum tsunami events and projected scenarios. The improved model employed in this study can be used to predict maximum run-up heights on coastal areas vulnerable to a tsunami attack. Predicted run-up heights can be used to construct an inundation map.

ACKNOWLEDGEMENTS

This research has been supported by the research grant from the Ministry of Maritime Affairs and Fisheries, Korea.

LITERATURE CITED

- CHO, Y.-S.; JIN, S.-B. and LEE, H.-J., 2004. Safety analysis of Ulchin Nuclear Power Plant against the Nihonkai-chubu Earthquake Tsunami. *Nuclear Engineering and Design*, Vol. 228, pp. 393-400.
- CHO, Y.-S. and YOON, S.-B., 1998. A modified leap-frog scheme for linear shallow-water equations. *Coastal Engineering Journal*, Vol. 40, No. 2, pp. 191-205.
- IMAMURA, F. and GOTO, C., 1988. Truncation error in numerical tsunami simulation by the finite difference method. *Coastal Engineering*, Vol. 31, pp. 245-263.
- LEE, H.-J., 1999. Study on Tsunami Hazards Mitigations Along the Korean eastern Coast. Research Report, NIDP-99-07. National Institute of Disaster Prevention, Korea (in Korean).
- LIU, P.L.-F.; CHO, Y.-S.; BRIGGS, M.J.; SYNOLAKIS, C.E. and KANOGLU, U., 1995. Run-up of solitary wave on a circular island. *Journal of Fluid Mechanics*, Vol. 302, pp. 259-285.
- LIU, P.L.-F.; CHO, Y.-S.; YOON, S.-B. And SEO, S.-N., 1995. Numerical simulations of the 1960 Chilean tsunami propagation and inundation at Hilo, Hawaii. In: Y. TSUCHIYA and N. SHUTO (ed.), *Tsunami: Progress in Prediction, Disaster Prevention and Warning. Advances in Natural and Technological Hazards Research*, Vol. 4, Kluwer Academic Press, pp. 99-115.
- MEI, C.C., 1989. *The Applied Dynamics of Ocean Surface Waves*. World Scientific Publishing Co, 740.
- SOHN, D.-H.; CHO, Y.-S.; HA, T.-M. and KIM, S.-M., 2006. A practical scheme for simulation of distant propagation of tsunami. India: Proceedings of the 15th Congress of Asia and Pacific Division of the International Association for Hydraulic Research and Engineering, pp. 1229-1235.
- WARMING, R.F. and HYETT, B.J., 1974. The modified equation approach to the stability and accuracy analysis of finite difference methods. *Journal of Computational Physics*, Vol. 14, pp. 159-179.